



Waviness Affects Friction and Abrasive Wear

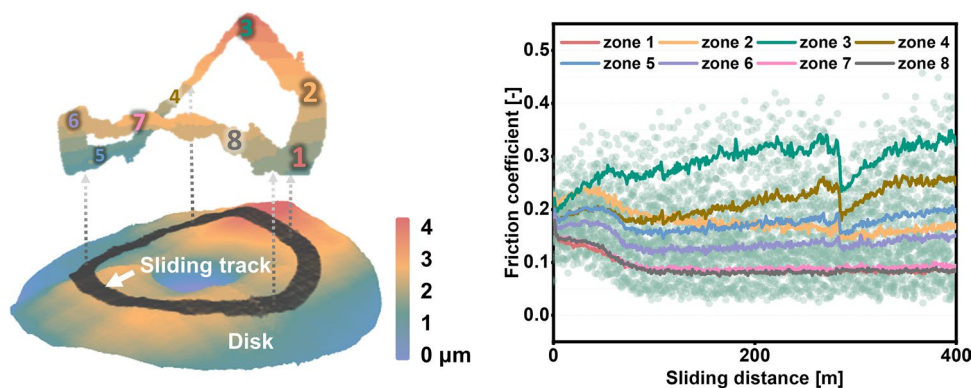
Yulong Li^{1,2} · Nikolay Garabedian^{1,2} · Johannes Schneider^{1,2} · Christian Greiner^{1,2}

Received: 21 February 2023 / Accepted: 11 April 2023 / Published online: 27 April 2023
© The Author(s) 2023

Abstract

Abrasive wear can have a detrimental effect on machinery, especially in the mining and construction industries. To prolong machinery lifetime and cut down energy consumption, a thorough understanding of abrasive wear is essential: surface topography measurement and interpretation (including form, waviness, and roughness) are vitally important. However, the potentially crucial influence of surface topography intricacies on tribological behavior has been obscured since roughness and waviness are considered simple scalar quantities in most cases (e.g., roughness R_a and waviness W_t). In this work, the complete waviness profile of the sliding track was used to shed light on the influence of surface topography on abrasive wear. Bearing steel (100Cr6, AISI 52100) pins and disks were tribologically tested in a flat-on-flat contact with Al_2O_3 -based slurries as interfacial medium. Using slurries with two different particle sizes, 5 and 13 μm , we found that friction fluctuates only with small abrasive particles (5- μm slurry) and relatively low waviness disks. It was found that even small surface deviations (albeit minimized and controlled for) can significantly increase the friction coefficient—up to 91%. Remarkably, not only are frictional fluctuations strongly correlated with the disk's initial waviness profile, but these small fluctuations correlate with unevenly distributed high wear. These findings enhance our understanding of the friction wear structure and provide the basis for exploring how surfaces can be optimized for better tribological performance.

Graphical Abstract



Keywords Abrasive wear · Surface topography · Friction fluctuation · Waviness · Roughness

✉ Christian Greiner
christian.greiner@kit.edu

¹ Institute for Applied Materials (IAM), Karlsruhe Institute of Technology (KIT), Kaiserstr. 12, 76131 Karlsruhe, Germany

² MicroTribology Center (μ TC), Strasse am Forum 5, 76131 Karlsruhe, Germany

1 Introduction

Undesirable abrasive wear is usually inevitable for machines, especially those operating in severe or contaminated conditions. Although researchers have produced sophisticated designs in lubrication, sealing, filtration, and other related fields, abrasive wear is still a vexing problem in practice. Aside from substantial carbon dioxide emissions due to high

friction and wear, remanufacturing and replacing worn-out parts incurs high economic losses and energy consumption [1–4].

Owing to the great importance of abrasive wear, extensive studies have been performed over the past decades by both academia and industry. Researchers traditionally classify abrasive wear mechanisms into “two-body abrasion” and “three-body abrasion” based on the operating conditions of abrasive particles and their influence on wear [5, 6]. Tribological performance and mechanism were found to be linked to additional parameters, e.g., type of abrasive [2], abrasive size [7–9], abrasive concentration [10], and load [11, 12]. Parallel wear grooves in the sliding direction and fluctuating friction have been widely reported in tribological studies as evidence of abrasive wear [13–21]. These parallel wear grooves are deemed a consequence of cutting and plowing due to passing abrasive particles [22–25]. The source of abrasive particles could be the breakdown of the contacting surfaces, filtering failure, the malfunction of sealing, lubricant starvation, as well as numerous others. However, to our best knowledge, the cause of fluctuating friction in abrasive wear has not yet been fully understood, even if friction fluctuations are a ubiquitous manifestation of abrasive wear.

In a tribological contact, surfaces are always intricate and usually defined via form, waviness, and roughness [26]—these surface irregularities have an influence on friction and wear. The effect of roughness on friction can be positively [27], negatively [28], or non-monotonically correlated [29]. Liang et al. [30] observed a drastic fluctuation in friction coefficient with the increase of R_a (average surface roughness). Due to the selection of different cut-off lengths for filtering the surface features of interest, surface roughness measurements commonly obscure the waviness portion of the surface profile [26]. Chang et al. [31] found that the waviness W_a (arithmetic average of surface heights, but at higher wavelengths than simple roughness) strongly correlates with friction between Neolite rubber and quarry tiles. However, the influence of waviness on tribological contacts is not broadly studied at present and has usually been overlooked.

As shown above, in most studies, the surface profile is characterized as mean roughness and waviness parameters, which are considered simple scalar quantities (e.g., roughness R_a and waviness W_t). These roughness and waviness parameters are not directly evaluated from the primary surface profile but generated from corresponding roughness and waviness profiles after filtering the primary profile in accordance with current standards (e.g., ISO 116610 or ASME B46.1). However, the actual surface topography is far more complicated than several scalars, which in turn may obscure the surface topography’s influence on tribological behavior. Even so, these quantitative indicators describing the surface topography have to be used in the surface

finishing process, as reaching a completely flat surface is almost impossible.

Given these quantification issues in surface topography and abrasive wear, we formulate a guiding question for this study: what is the systematic relationship between friction fluctuation, surface topography, and wear? In our study, instead of using quantitative indicators (e.g., R_a and W_t), the complete waviness profile along the sliding track is used to evaluate the tribological behavior. The circular sliding track was subdivided into small segments, and the tribological data were evaluated for each of these segments and every revolution of the disk in our pin-on-disk experiments. The friction along the sliding track was then compared with the waviness profile and wear distribution. Our results strongly suggest that frictional fluctuations strongly correlate with the waviness profile and also result in uneven wear.

2 Materials and Methods

2.1 Materials

Bearing steel (100Cr6, AISI 52100) was chosen as pin and disk material for the pin-on-disk configuration. The pins were purchased from KGM (Fulda, Germany) with a nominal hardness of 700 HV, roughness values of $R_a = 0.02\text{--}0.04\ \mu\text{m}$, and a total waviness profile height $W_t \leq 0.6\ \mu\text{m}$ (identical with the ISO 4287, measured by HOMMEL-ETAMIC T8000 R120-400 tactile surface profilometer, Villingen-Schwenningen, Germany). The 8-mm-diameter sphere pins were flattened on one side to a circular area (diameter 7.3 mm) by grinding and polishing. The material for the 70-mm-diameter bearing steel disks was obtained from Eisen Schmitt (Karlsruhe, Germany) and then hardened and tempered to a hardness of approx. 800 HV. The surface preparation of the disk was done by grinding with corundum grinding wheels of grit EK200 (G&N MPS 2 R300, Erlangen, Germany) to a roughness ranging from $R_a = 0.08\text{--}0.12\ \mu\text{m}$. The total waviness profile height W_t (based on ISO 4287) along the sliding track was specifically paid attention to with an optical surface profilometer (FRT MicroProf MPR 1024, Bergisch Gladbach, Germany), with a reference value of $W_t \leq 2\ \mu\text{m}$. Water-based Al_2O_3 abrasive slurries with two different particle sizes (Lapping medium BIOLAM®; 5 μm and 13 μm based on FEPA grains standard) were obtained from Joke (Bergisch Gladbach, Germany). A laser granulometry (CILAS 1064, Orléans, France) was employed to measure the size distribution of Al_2O_3 in slurries, and the results can be seen in Fig. S1 [19]. The concentration of Al_2O_3 in the slurries is 12.5 wt%.

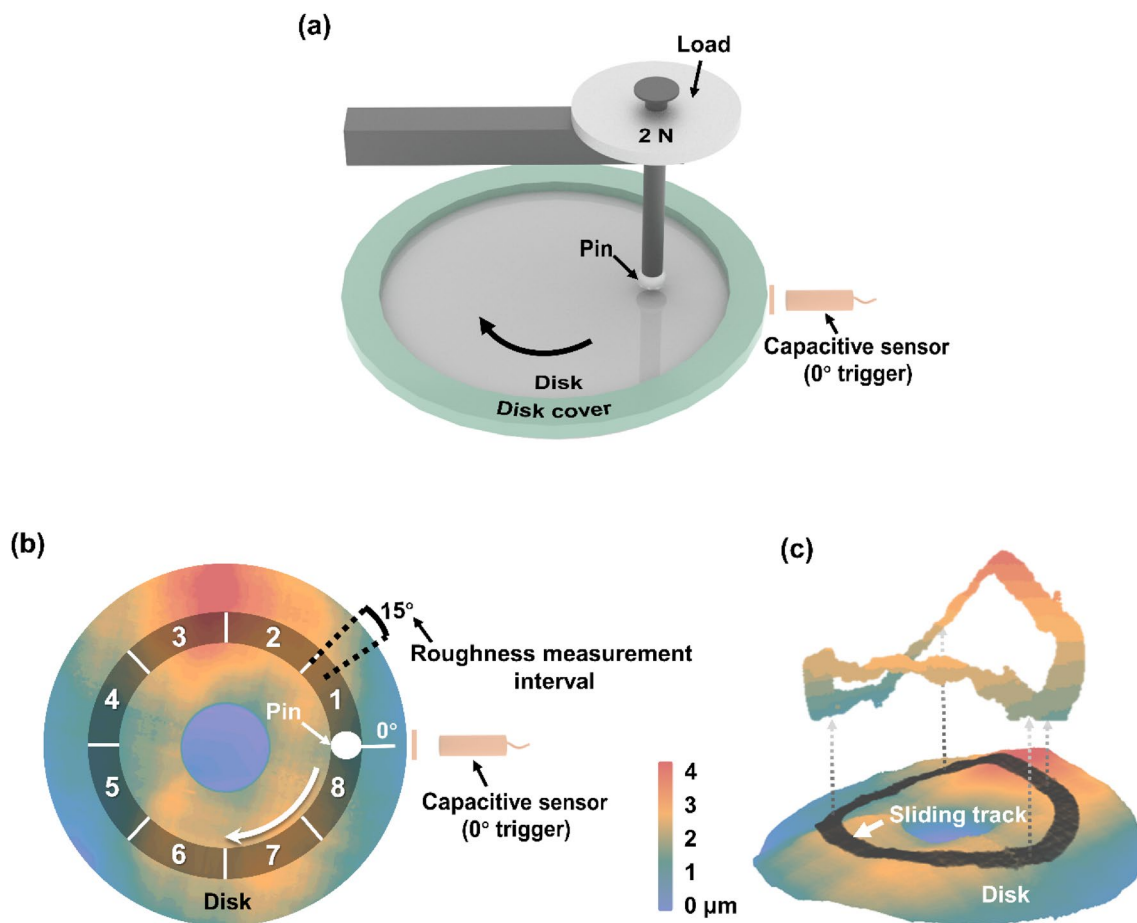


Fig. 1 **a** Schematic of the pin-on-disk tribology test; the disk rotates clockwise. **b** Top view schematic, separating the tribological data into 8 zones with respect to the 0° triggered by the capacitive sensor, and

roughness measurement with every 15-degree interval on the disks' sliding track; **c** Extracting the surface profile of the 7.33-mm width sliding track from optical surface profilometry data

Table 1 Experiments and their settings

	Slurry size (μm)	W_t (Total height of the waviness profile)	Sliding distance (m)
5_S	5	$\leq 2 \mu\text{m}$	846
5_S_50	5	$\leq 2 \mu\text{m}$	50
13_S	13	$\leq 2 \mu\text{m}$	846
13_L	13	$\geq 7 \mu\text{m}$	846

2.2 Tribological Testing

Pin-on-disk tests were carried out with a CSEM tribometer (CSM Instruments, Peseux, Switzerland, now owned by Anton Paar). In order to segment the data from each disk revolution, a capacitive sensor and a metallic block flag were mounted on the tribometer, as shown in Fig. 1a. The zero position of every circle was triggered with data from the capacitive sensor activated by the metallic block coaxial

moving with the disk, as shown in Fig. 1b. The tribological tests were performed at 50 mm/s with a 50-Hz sampling rate; thus, the resolution of the data acquisition is 1 mm along the sliding direction (132-mm total sliding track per revolution). The normal force was 2 N for all experiments, and the friction force was measured through the loading arm's deflection. A 21-mm sliding radius was chosen to minimize the influence of a velocity gradient in a flat-on-flat contact [31]. For each test, 100 ml of slurry was added to the experimental setup before the experiment in order to ensure bath-like conditions around the contacting surfaces throughout the entire experiment.

Four kinds of experimental settings were tested, as shown in Table 1. Tribological tests 5_S and 5_S_50 were performed with the 5- μm slurry, while 13_S and 13_L were tested with the 13- μm slurry. 5_S, 5_S_50, and 13_S were prepared with a small waviness, where W_t is less than or equal to 2 μm . 13_L has a deliberately larger waviness of $W_t \geq 7 \mu\text{m}$. The sliding distance was 846 m for all experiments except for one with 50 m (5_S_50). This experiment

was shortened so that we could examine the surface's transient state. The experimental settings for 5_S and 13_S were repeated three times and each with fresh samples; 5_S_50 and 13_L were performed only once.

2.3 Data Evaluation and Characterization

Worn surfaces of the disk were examined using an FEI Helios NanoLab 650 dual-beam scanning electron microscope (FEI Company, USA). The roughness distribution was measured radially every 15 degrees of the sliding track with a stylus profilometer HOMMEL-ETAMIC T8000 R120-400 (schematic in Fig. 1b). These roughness measurements were performed for all disks before and after the tribological tests. Before the tribological experiments, roughness measurements were performed tangentially to the sliding direction, with the aim of achieving as perpendicular a measurement direction as possible relative to the grooves created by grinding. In contrast, after the tribological tests, the roughness was measured radially, guaranteeing that these measurements were performed perpendicular to the sliding direction.

Additionally, the waviness profile and wear volume were determined via optical surface profilometry measured with a FRT MicroProf optical surface profilometer. Taking these images, first, the surface profile along the sliding track was extracted from the optical profilometry data, as shown in Fig. 1c. The surface profile was then divided into 120 ring segments, with each segment covering 3° of the total circumference (width of 7.33 mm, centered at 21 mm radius). The waviness profile was evaluated from the surface profile by averaging the height of each segment and following with a profile filtering with cut-off length $\lambda_c = 0.08$ mm (in accordance with ISO 16610). The average value of each segment is the average for the following 3 degrees, e.g., the value at $x = 0^\circ$ is the average of the value from 0 to 3° . The amount of wear along the sliding track is calculated by comparing the surface topography before and after the experiments.

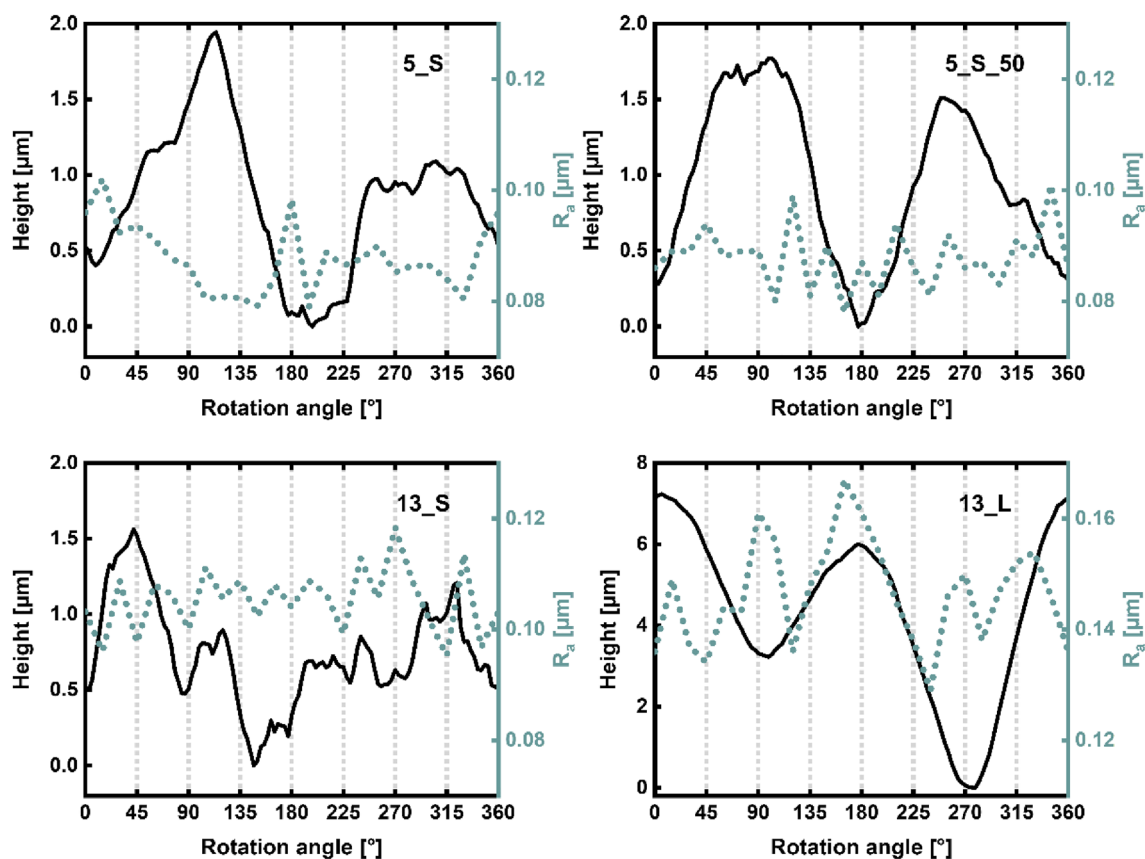


Fig. 2 Waviness profile and roughness distribution along the sliding track for four individual disks: 5_S, tested with 5- μm slurry and small waviness; 5_S_50, tested with 5- μm slurry and small waviness for

a short sliding distance (50 m); 13_S, tested with 13- μm slurry and small waviness; 13_L, tested with 13- μm slurry and large waviness

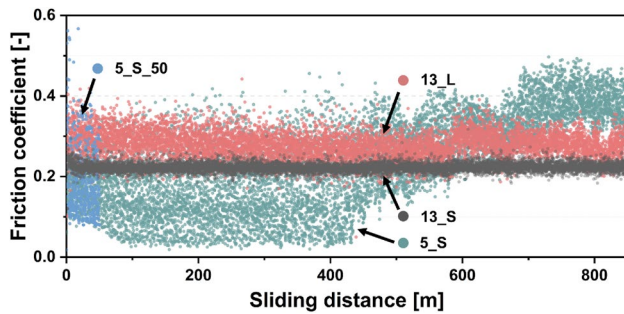


Fig. 3 Friction coefficient from four experimental settings: 5_S, tested with 5- μm slurry and small waviness; 5_S_50, tested with 5- μm slurry and small waviness for a short distance (50 m); 13_S, tested with 13- μm slurry and small waviness; 13_L, tested with 13- μm slurry and large waviness

3 Results

3.1 Waviness Profile

Figure 2 displays the waviness profile and roughness distribution along the sliding track for four disks, which were then tested with corresponding settings presented in Table 1. There are three repeats for 5_S and 13_S, which are not discussed in the main body of paper and can be seen in the supplemental materials. For the considered specific disks with a small waviness (5_S, 5_S_50, and 13_S), the total height of the profile W_t along the sliding track is 1.94 μm , 1.77 μm , and 1.56 μm , respectively. However, even with the same waviness standard ($W_t \leq 2 \mu\text{m}$), the waviness profiles of 5_S, 5_S_50, and 13_S differ significantly from each other. Two clear peaks can be seen for both 5_S and 5_S_50. 5_S shows a sharp peak (around 110°) considerably higher than another peak (between 230° and 300°) in 5_S, while the heights of the peaks in 5_S_50 is very close. Unlike 5_S and Disk 5_S_50, 13_S does not have significant high peaks, but several small peaks can be viewed along the sliding track. The waviness of 13_L was intentionally not mitigated during the grinding process, which yielded a total waviness profile height of $W_t = 7.24 \mu\text{m}$. The roughness R_a along the sliding track of the disks with a small waviness (5_S, 5_S_50, and 13_S) ranges from 0.08 to 0.12 μm , with average values of 0.09 μm , 0.09 μm , and 0.11 μm , respectively. 13_L has a slightly higher average roughness, $R_a = 0.15 \mu\text{m}$. Similar to the waviness profiles, the roughness distribution along the sliding track varies from disk to disk.

3.2 Friction

The results for the friction coefficient as a function of the sliding distance for all tests are presented in Fig. 3. No smoothing or averaging was applied to these data, and for visualization purposes, only the first out of every 100 data

points is displayed; the evaluations in all later parts, however, are based on the entire data obtained at a 50-Hz sampling rate. The data shown here give an overview of the friction coefficient as well as the influence of the abrasive particle size. For the experiments with the 5- μm slurry, small disk waviness, and 846-m sliding distance (5_S), friction fluctuations appear from the beginning (0–50 m) of the test, ranging from 0.1 to 0.3. An increase in friction coefficient can be noticed after 400 m; the friction coefficient increases and then oscillates between 0.2 and 0.5. It is worth noting that although frictional fluctuations drop slightly with sliding distance, they are still considerable (around 0.2). The result of 5_S_50 (tested with 5- μm slurry and small waviness for a shorter distance of 50 m) shows a similar trend to 5_S; frictional fluctuations start from the beginning of the test, ranging from 0.1 to 0.5.

The friction coefficient for the experiments with 13- μm slurry and a small disk waviness (13_S in Fig. 3) exhibits a different trend than the experiments with 5- μm slurry and small waviness (5_S and 5_S_50 in Fig. 3). The friction coefficient is relatively stable for 13_S, apart from a slight decrease in friction coefficient for the first 20 m, fluctuation mainly ranging from 0.2 to 0.25. The fluctuation in friction coefficient for the experiment with 13- μm slurry and a small disk waviness (13_S) is less than 1/5 compared to the tests performed with the 5- μm slurry (5_S and 5_S_50). The average friction coefficient for the experiment with 13- μm slurry and a small disk waviness (13_S) is $\mu = 0.22$, a bit lower than that for the experiment with 13- μm slurry and increased disk waviness of around 7 μm (13_L), $\mu = 0.28$. Moreover, 13_L has a more significant fluctuation in friction coefficient (mainly ranging from 0.2 to 0.4) than 13_S (mainly ranging from 0.2 to 0.25).

With the tribometer in Fig. 1 and a sampling rate of 50 Hz, the tribological data can be divided into eight zones of 45-degree intervals (schematic in Fig. 1b). Hence, it is feasible to average the friction coefficient in each zone, as shown in Fig. 1b. For the result of the experiment with 5- μm slurry and a small disk waviness (5_S in Fig. 4), the friction coefficient in zone 3 is relatively high (average $\mu = 0.33$) and low friction coefficient appears in zone 1 and 8 (average $\mu = 0.18$). Similar to 5_S, the difference in friction coefficient between the individual zones can be distinguished from 5_S_50 in Figure S2. The maximum difference in friction coefficient between each zone can be up to 0.2 for 5_S and 5_S_50, but 13_L is less prominent and here the value is only 0.04. In marked contrast to the experiment with the 5- μm slurry and a small disk waviness (5_S and 5_S_50), the friction coefficient of each zone for the experiment with 13- μm slurry and a small disk waviness (13_S in Fig. 4) does show only very little difference.

Fig. 4 Friction coefficient on the disk is divided into eight zones: 5_S, tested with 5- μm slurry and small waviness; 13_S, tested with 13- μm slurry and small waviness; and 13_L, tested with 13- μm slurry and large waviness

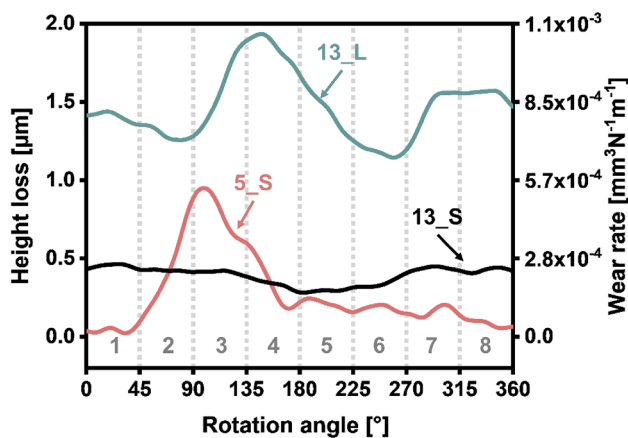
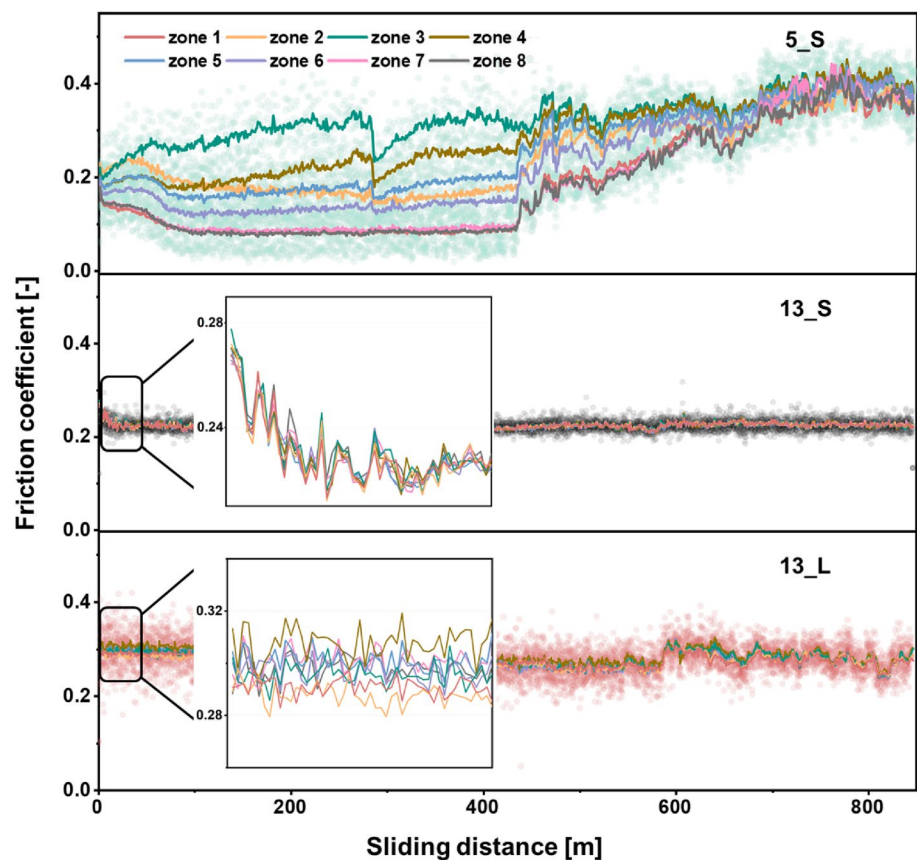


Fig. 5 Wear-induced height loss and wear rate along the sliding track: 5_S, tested with 5- μm slurry and small waviness; 13_S, tested with 13- μm slurry and small waviness; and 13_L, tested with 13- μm slurry and large waviness

3.3 Wear

In Fig. 5, the wear-induced height losses and the wear rate for the experiments with the 5- μm slurry and a small disk waviness (5_S), the 13- μm slurry and a small disk waviness

(13_S), and the 13- μm slurry and a large disk waviness (13_L) are shown. The wear rate was evaluated based on Archard's wear equation [32]. The average wear along the sliding track for 5_S, 13_S, and 13_L was found to be 0.39 μm , 0.31 μm , and 1.47 μm , respectively. Correspondingly, the average wear rates were calculated to be $2.2 \times 10^{-4} \text{ mm}^3/\text{Nm}$, $1.8 \times 10^{-4} \text{ mm}^3/\text{Nm}$, and $8.4 \times 10^{-4} \text{ mm}^3/\text{Nm}$. For 13_S, the height loss on the frictional track ranges from 0.28 μm to 0.46 μm , with high wear around 0° and low wear around 180° . A significantly different behavior can be noticed for 5_S and 13_L; the wear distribution along the sliding track is uneven. For 5_S, almost no height loss is present around 0° , whereas the height loss is close to 1 μm around 110° . Rotation angles between 60° and 160° contribute almost 2/3 of the wear. Uneven wear also occurs in 13_L: Around 150° , the height loss is up to 1.93 μm , while the lowest height loss appears around 270° (about 1.15 μm).

3.4 Worn Surfaces

Figure 6 presents SEM images of the areas with the highest and lowest friction coefficients for experiments tested with 5- μm slurry (5_S and 5_S_50) and 13- μm slurry with large waviness (13_L). The SEM images of worn surfaces were all taken in the middle of the sliding track. For 5_S,

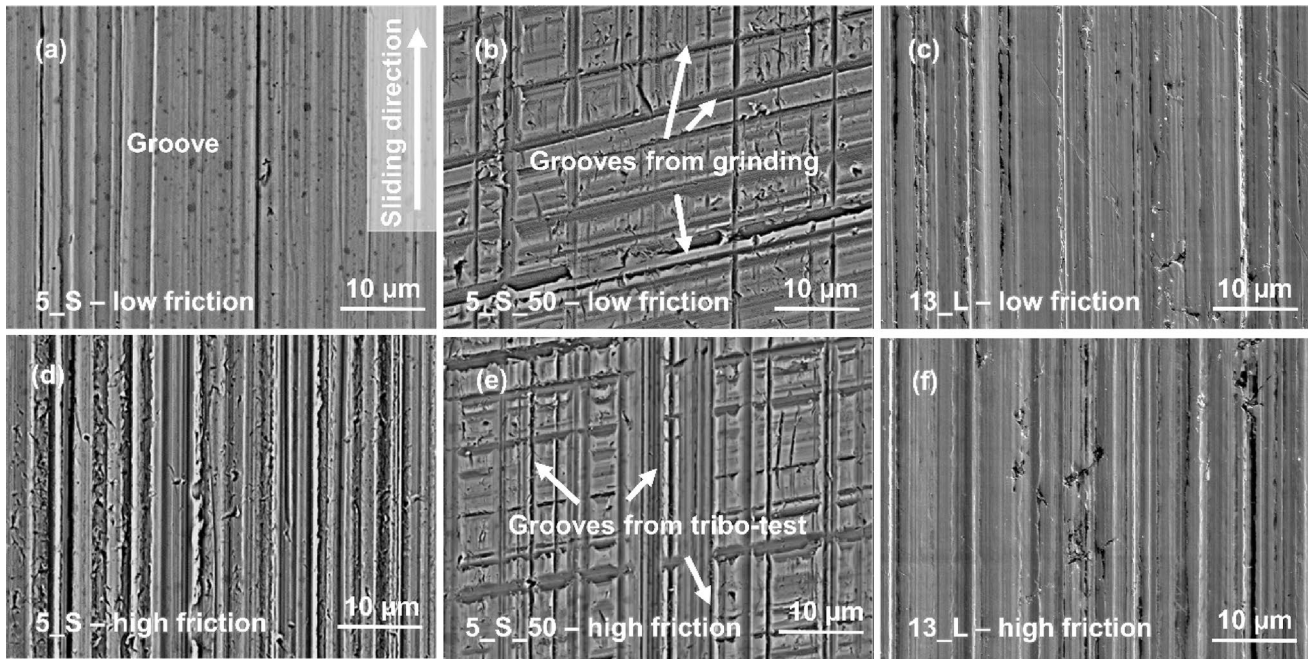


Fig. 6 SEM images of the worn surfaces at different areas on the sliding track: **a** and **d** tested with 5- μm slurry and small waviness (5_S), (**a**) is the low friction area around 0° (the boundary between zone 1 and zone 8) and **d** is the high friction area around 110° (zone 3); **b** and **e** tested with 5- μm slurry and small waviness for a short distance

(50 m), **b** is the low friction area around 110° (zone 3) and **e** is the high friction area around 300° (zone 7); **c** and **f** tested with 13- μm slurry and large waviness, **c** is the low friction area around 70° (zone 2) and **f** is the high friction area around 150° (zone 4)

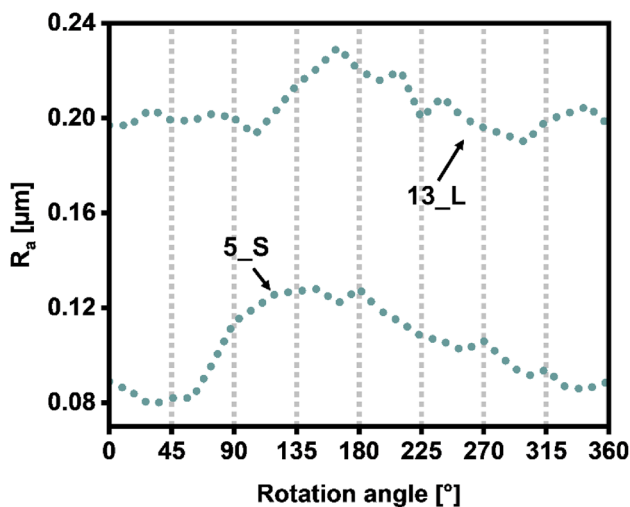


Fig. 7 Roughness distribution along the sliding track after the tribological tests: 5_S, tested with the 5- μm slurry and small waviness; 13_L, tested with the 13- μm slurry and large waviness

grooves appear in both the high friction area (Fig. 6a, corresponds to zone 3, around 110°) and the low friction area (Fig. 6c). The grooves in the high friction area are more pronounced than those in the low friction area. The contrast in the worn surfaces of different zones also appears

for 5_S_50 (Fig. 6b, d). The test of 5_S_50 was performed for 50 m, so the vestiges of the surface preparation still exist in the wear track (the grooves vertical or approximately vertical to the sliding direction). For the grooves generated during the tribological experiments, the high friction area (Fig. 6e) of 5_S_50 has more distinct grooves than the low friction area (Fig. 6b). The grooves do not have a significant difference for the high friction area and the low friction area of 13_L, in Fig. 6c and f.

3.5 Worn Roughness

The feedback between the friction coefficient and the roughness distribution along the sliding track for 5_S (tested with 5- μm slurry and a small disk waviness) and 13_L (tested with 13- μm slurry and a large disk waviness) are highlighted in Fig. 7. Here, the roughness measurements were performed on the sliding track after the tribological tests. For 5_S, the roughness R_a along the sliding track ranges from 0.08 μm to 0.13 μm , with an average value of 0.10 μm . 13_L has a relatively larger roughness R_a ranging from 0.19 μm to 0.23 μm , with average roughness $R_a = 0.20 \mu\text{m}$.

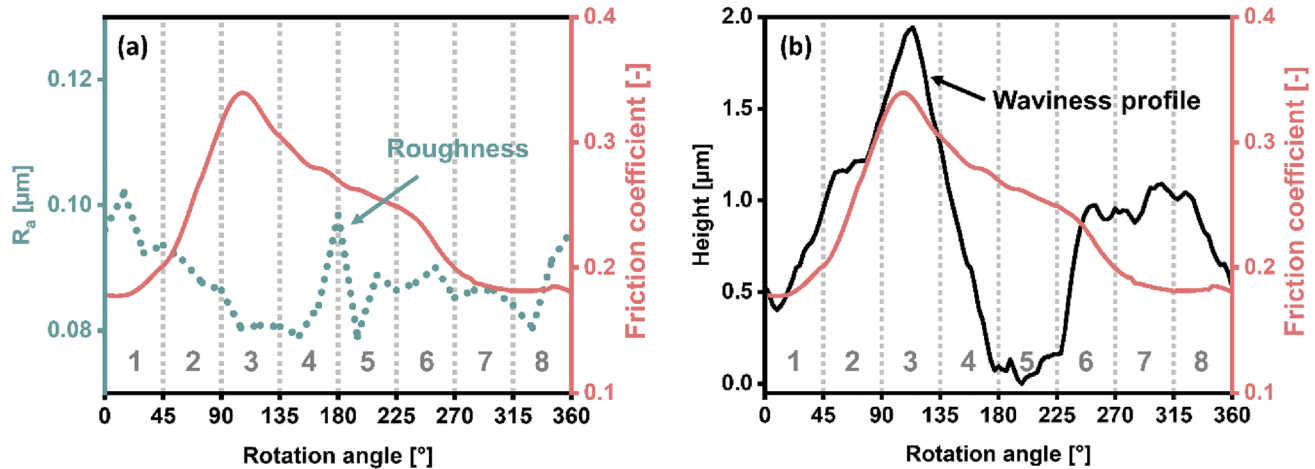


Fig. 8 Comparing friction coefficient (in Fig. 4) with roughness distribution and waviness profile (in Fig. 2) for 5_S, tested with the 5- μm slurry and small waviness: **a** friction coefficient & roughness distribution and **b** friction coefficient & waviness profile

4 Discussion

In line with previous reports [17, 20, 21], friction coefficient fluctuations occur with abrasive wear in our study (5_S, 5_S_50, and 13_L in Fig. 3). The waviness profile, roughness distribution, and wear along the sliding track were successfully obtained from optical surface profilometry data. In the discussion, the reason for the friction coefficient fluctuations is addressed first; then, the distribution of friction coefficient along the sliding track will be directly compared to the roughness distribution, waviness profile, and wear. The main focus of this study is to investigate the impact of disk waviness on the tribological behavior. Therefore, the pin was held to rigorous standards and constant, and it is therefore considered a stable factor when interpreting the experimental results. To the best of our knowledge and by having a rigorous look at all data gathered throughout these experiments, this is a reasonable assumption. At the same time, it is an assumption and future research might have to address the pin side of the tribological system systematically.

The tribological data of the experiments can be divided into eight zones, as shown in Fig. 4. The results strongly suggested that fluctuations in friction coefficient for experiments tested with 5- μm slurry and a small waviness (5_S), 5- μm slurry and small waviness for a short distance (5_S_50), and 13- μm slurry and a large waviness (13_L) are due to inconstant friction coefficient along the sliding track. Some areas on the disk obviously lead to a higher friction, for example, zone 3 on 5_S; some areas result in a locally lower friction, e.g., zones 7 and 8 on 5_S. The inconstant friction coefficient along the sliding track on pin-on-disk setups has not been a focus of attention in most tribological studies, and few publications reported this phenomenon and even when they do, they do not point out the cause [33–35].

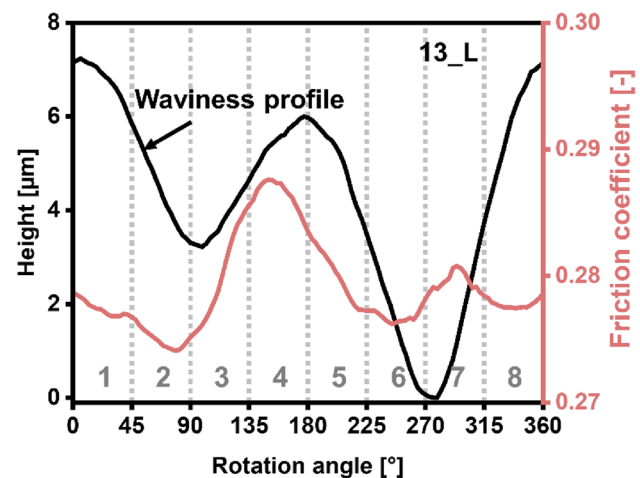


Fig. 9 Comparing the waviness profile in Fig. 2 and the friction coefficient in Fig. 4 for 13_L, tested with the 13- μm slurry and large waviness

To elucidate what could be the reason for inconstant friction along the sliding track of 5_S, in Fig. 8, the average friction coefficient along the entire wear track (in Fig. 4) is compared to the roughness distribution and waviness profile (in Fig. 2), respectively. The entire sliding track (360°) is divided equally into 120 segments when evaluating the average friction coefficient, and the average friction coefficient of each segment is the average for the next 3° degrees. e.g., the friction coefficient at $x = 0^\circ$ (as plotted) is the average friction coefficient between 0° and 3° .

For 5_S (Fig. 8a), there is no visible correlation between friction coefficient and roughness. By contrast, there is partial correlation between friction coefficient and waviness profile in Fig. 8b. The friction coefficient is the highest

where the waviness profile has its maximum height; a “hill” of around $2\ \mu\text{m}$ height can increase the friction coefficient by 91%. Similar results are obtained when testing with a $5\text{-}\mu\text{m}$ slurry and small waviness for a short distance (5_S_50 in Figure S3) and $13\text{-}\mu\text{m}$ slurry and a large waviness (13_L in Fig. 9). It seems that in the circumstances of lubricated abrasive wear, higher friction (zone 3, around 110° in Fig. 8) is correlated with regions experiencing more aggressive abrasion (Fig. 6d). This most likely is due to an increased occurrence of two-body abrasion, while the abrasive gets embedded in the softer pin. The influence of the waviness profile on friction behavior is consistent with results published by Dai et al. [36] in molecular dynamics simulations, where they studied the molecular structure, deformation, and friction at the sliding interface between a ta-C tip and heterogeneous polymer (perfluoropolyether) surfaces; the friction force increased sharply when the probe tip overcame surface pile-ups.

In Dai et al.’s study, the maximum total height difference is $0.2\ \text{nm}$ in a 30-nm sliding track (with a height-to-length

ratio of 0.07). However, the ratio in our experiment is only 1.5×10^{-5} ($2\ \mu\text{m}$ in $132\ \text{mm}$). For a steel surface, controlling the height difference to less than $2\ \mu\text{m}$ on such a long sliding track ($132\ \text{mm}$) is no easy matter. Therefore, it is astonishing to find that such a tiny height difference in the waviness profile hugely influences abrasive wear.

When making use of disks with a small waviness ($W_t \leq 2\ \mu\text{m}$), fluctuations in friction coefficient were only observed for experiments with the $5\text{-}\mu\text{m}$ slurry (5_S and 5_S_50 in Fig. 3), while the friction coefficient in experiments with the $13\text{-}\mu\text{m}$ slurry (13_S in Fig. 3) is more stable. Consistent with this observation, the results of repeated experiments for 5_S and 13_S can be found in Figure S4. The question therefore arises whether this behavior is caused by the fact that smaller slurry particles are more sensitive to the waviness profile, thereby leading to higher fluctuation in friction coefficient. With this question in mind, base bodies (e.g., 13_L) with intentionally higher waviness ($W_t = 7.24\ \mu\text{m}$) were tested with the $13\text{-}\mu\text{m}$ slurry. By comparing the average friction coefficient along the sliding track

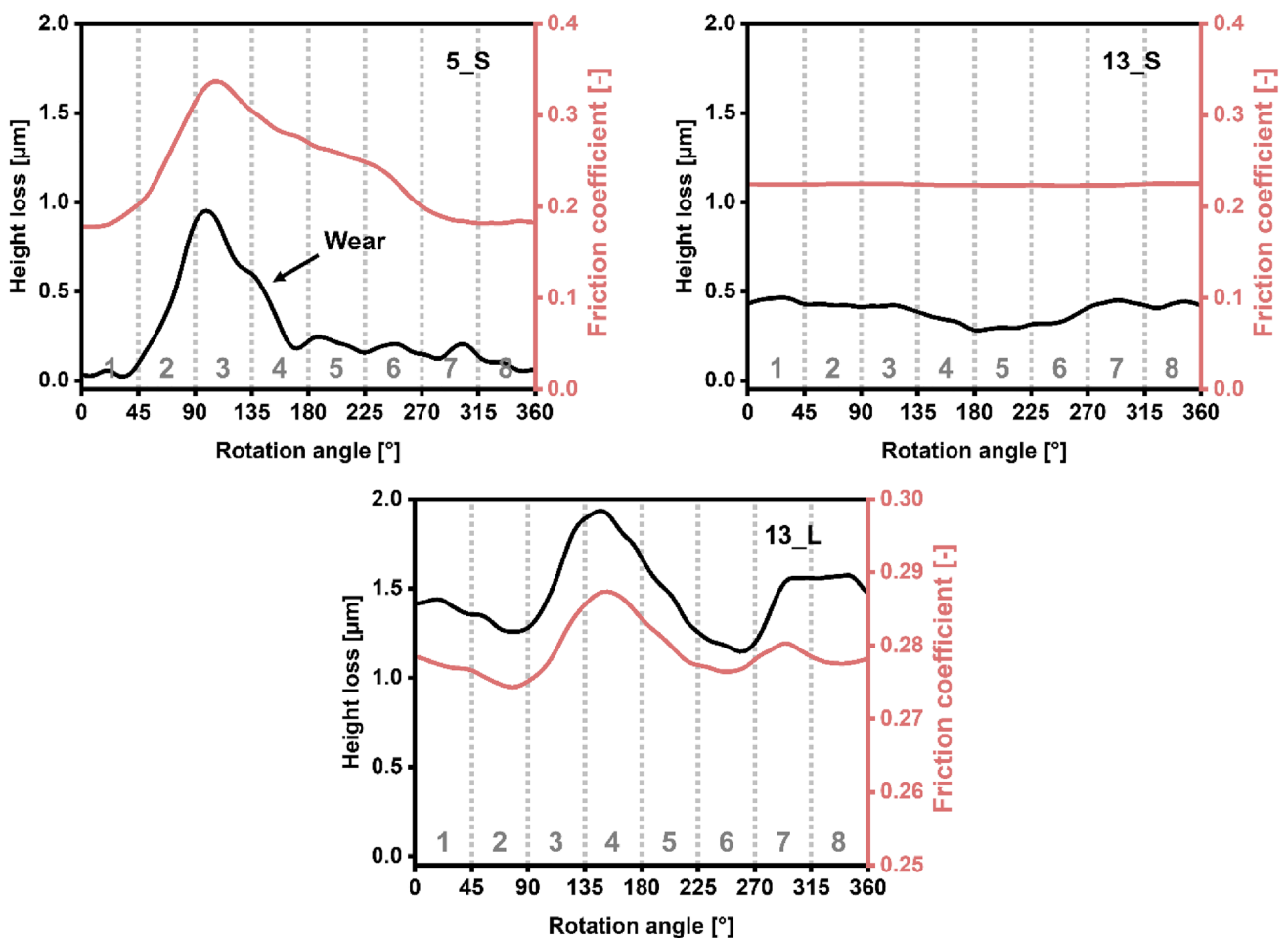


Fig. 10 Comparing friction coefficient (from Fig. 4) with wear-induced height loss (from Fig. 5) for 5_S, tested with the $5\text{-}\mu\text{m}$ slurry and small waviness; 13_S, tested with the $13\text{-}\mu\text{m}$ slurry and small waviness; and 13_L, tested with the $13\text{-}\mu\text{m}$ slurry and large waviness

and the waviness profile for the experiments conducted with the 13- μm slurry and increased waviness (13_L), one can infer that at locations on the disks where the waviness profile shows a positive slope (of the “hills”), the friction coefficient also increases. When W_t is increased from 1.56 μm (13_S) to 7.24 μm (13_L), the base bodies’ waviness profiles not only show an influence on the friction behavior when tested with the 13- μm slurry, but also the wear rate significantly increased from $1.8 \times 10^{-4} \text{ mm}^3/\text{Nm}$ to $8.4 \times 10^{-4} \text{ mm}^3/\text{Nm}$ (see Fig. 5). This underlines that for abrasive conditions with small abrasive particles (5- μm slurry), the waviness profile has a much more pronounced influence compared to systems where the abrasive particles are larger (13- μm slurry). A critical ratio between the waviness profile W_t and particle size might exist, making it even possible to predict the onset of considerable fluctuation in friction coefficient. It is therefore a possible avenue for future research in the field of abrasive wear.

In most simple terms, friction often has a strong influence on wear during tribological loading [37]; consequently, friction fluctuations might also influence wear. In Fig. 5, the wear of 5_S (tested with 5- μm slurry and a small disk waviness) and 13_L (tested with 13- μm slurry and a large disk waviness) is more uneven than that of 13_S (tested with 13- μm slurry and a small disk waviness). To elucidate the relationship between fluctuations in friction coefficient and uneven wear along the sliding track, the wear-induced height loss along the sliding track (Fig. 5) is directly compared to the friction coefficient for 5_S, 13_S, and 13_L (Fig. 4) in Fig. 10. For 5_S and 13_L, it is apparent that most of the wear occurred in the areas with the highest friction coefficient. There is a very clear and close correlation between the friction coefficient and the height loss in both cases. In contrast, for 13_S, the friction coefficient is almost constant over the entire

sliding radius, and the same can—with a grain of salt—also be said about the height loss. These results indicate that fluctuations in friction, together with increased base body waviness, correlate with uneven wear along the sliding track.

In Fig. 11, the friction coefficient for the last 50 m of the tests (790–840 m, Fig. 4) and the roughness R_a along the sliding track after the test (Fig. 7) are compared for 5_S and 13_L. A clear correlation can be seen in this figure between in-track roughness distribution and friction coefficient. An intricate feedback mechanism seems to exist between waviness, wear, friction coefficient, and surface roughness. The SEM images of the worn surfaces presented in Fig. 6 also support this line of thought. For experiments tested with a 5- μm slurry and small waviness (5_S), the portion of the disk with a higher friction coefficient (around 110°) shows more distinct grooves than the parts of the disk with a lower average friction coefficient (around 0°), which also correlates with the roughness profile presented in Fig. 11. This difference in surface morphology can be observed from early on in the tests (5_S_50, 50 m, Fig. 6b) and until the end of the experiments (5_S, 846 m, Fig. 6c). In contrast and owing to the stable friction coefficient of experiments tested with 13- μm slurry and small waviness (13_S), the worn surface in different areas shows very little difference (see Figure S5). For 13_L, the worn surfaces in high friction and low friction zones also do not show significant differences; this might be due to the fact that the friction differences in these regions are not as large as for 5_S and 5_S_50 and therefore do not cause significantly different worn surfaces. This is another indication that fluctuations in friction coefficient result in differently worn surfaces.

Owing to the complexity of any surface profile, simple scalar quantities like R_a and W_t can only be first-order approximations when it comes to the effect that the whole

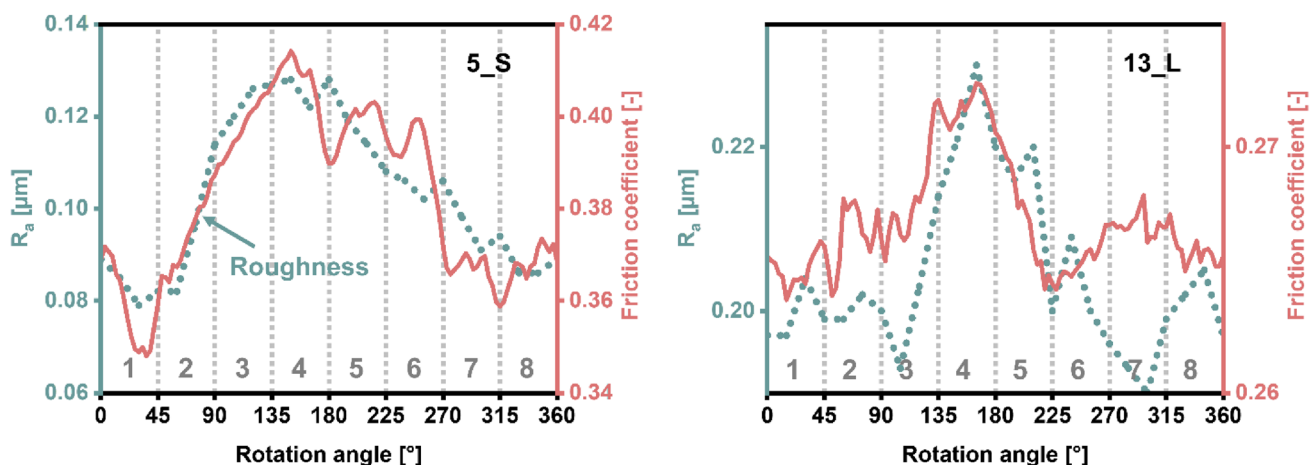


Fig. 11 Comparing roughness R_a along the sliding track after test (Fig. 7) and friction coefficient in the later phases (790–840 m in Fig. 4): 5_S, tested with the 5- μm slurry and small waviness; 13_L, tested with the 13- μm slurry and large waviness

profile has in the properties of the tribological system, even if these scalar quantities (e.g., R_a and W_l) are commonly used to define surface condition during a manufacturing process. By directly comparing the waviness profile to the tribological data, we could shed light on a previously overlooked aspect in terms of the influence of waviness on the tribological response. The data strongly suggested that apparent friction coefficient fluctuations are the result of variable friction coefficients along the sliding track, which are interrelated to the waviness profile, and eventually, lead to uneven wear. However, current surface finishing technology cannot reliably reproduce identical surface profiles, and this limits the utilization of the variable-control approach. Painting a complete picture of waviness influences [38] would require a large quantity of high-quality data which cannot be easily gathered by isolated groups and instead needs the contribution of the larger portions of the tribology community.

5 Conclusion

By adding a zero position trigger on a pin-on-disk tribometer, the tribological data were separated for each revolution and specific areas could be evaluated. The friction coefficient along the sliding track was then compared with the complete waviness profile, roughness distribution, and wear along the sliding track instead of using quantitative indicators. The data clearly demonstrates a relationship between friction fluctuations, waviness profile, and wear. Our results and their critical discussion allow us to draw the following conclusions:

- The waviness profile of the moving base body, in our case bearing steel disks, strongly influences the friction behavior. Even small deviations in the surface profile, e.g., a “hill” of around 2 μm height (along the 132-mm sliding track), can increase the friction coefficient by 91%. The local difference in friction coefficient is the reason behind the large scatter in friction data often observed in abrasive wear conditions.
- Tribological systems with smaller abrasive particles (e.g., in 5- μm slurry) are more sensitive to the waviness profile than systems with larger particles (e.g., in 13- μm slurry). As the waviness profile gets more pronounced; however, the influence of the waviness manifests itself for larger particles too.
- The local fluctuation in the friction coefficient results in uneven wear along the wear track. There is a clear, positive correlation between the local friction coefficient and the local wear.

Along with wear being affected by the waviness profile, through the friction coefficient, also the local surface

roughness shows a very similar positive correlation with the waviness profile. This clearly shows the dramatic influence of the base bodies’ local waviness profile on friction, wear, and surface roughness present for abrasive wear conditions, an important factor that previously seems not to have gotten the attention it deserves and that should be taken into account in future.

Supplementary Information The online version contains supplementary material available at <https://doi.org/10.1007/s11249-023-01736-1>.

Acknowledgements Christian Greiner acknowledges funding by the European Research Council (ERC) under Grant No. 771237, TriboKey. Yulong Li thanks the funding by China Scholarship Council (CSC). Nikolay Garabedian acknowledges the postdoctoral fellowship by the Alexander von Humboldt Foundation.

Author Contributions YL: Investigation (lead), Methodology (equal), Writing – Original Draft Preparation (lead); NG: Methodology (equal), Supervision (equal), Visualization (supporting), Writing - Review & Editing (equal); JS: Supervision (equal), Writing - Review & Editing (equal); CG: Conceptualization (lead), Methodology (equal), Writing - Review & Editing (equal).

Funding Open Access funding enabled and organized by Projekt DEAL. This study was supported by China Scholarship Council, Alexander von Humboldt-Stiftung, H2020 European Research Council (Grant No. 771237, TriboKey).

Data Availability The data used in this research is available upon request. Please contact the corresponding author for access to the data.

Declarations

Conflict of interest The authors declare that they have no conflict of interest.

Open Access This article is licensed under a Creative Commons Attribution 4.0 International License, which permits use, sharing, adaptation, distribution and reproduction in any medium or format, as long as you give appropriate credit to the original author(s) and the source, provide a link to the Creative Commons licence, and indicate if changes were made. The images or other third party material in this article are included in the article's Creative Commons licence, unless indicated otherwise in a credit line to the material. If material is not included in the article's Creative Commons licence and your intended use is not permitted by statutory regulation or exceeds the permitted use, you will need to obtain permission directly from the copyright holder. To view a copy of this licence, visit <http://creativecommons.org/licenses/by/4.0/>.

References

1. Holmberg, K., Kivikytö-Reponen, P., Härkisaari, P., Valtonen, K., Erdemir, A.: Global energy consumption due to friction and wear in the mining industry. *Tribol. Int.* (2017). <https://doi.org/10.1016/j.triboint.2017.05.010>
2. Petrica, M., Badisch, E., Peinsitt, T.: Abrasive wear mechanisms and their relation to rock properties. *Wear* (2013). <https://doi.org/10.1016/j.wear.2013.10.005>
3. Wang, L., Qiao, Z., Qi, Q., Yu, Y., Li, T., Liu, X., Huang, Z., Tang, H., Liu, W.: Improving abrasive wear resistance of Si3N4

- ceramics with self-matching through tungsten induced tribochemical wear. *Wear* (2022). <https://doi.org/10.1016/j.wear.2022.204254>
4. Stachowiak, G.W., Batchelor, A.W. (eds.): Butterworth-Heinemann, Boston (2014)
 5. Misra, A., Finnie, I.: A review of the abrasive wear of metals. *J. Eng. Mater. Technol.* (1982). <https://doi.org/10.1115/1.3225058>
 6. Rabinowicz, E., Dunn, L.A., Russell, P.G.: A study of abrasive wear under three-body conditions. *Wear* (1961). [https://doi.org/10.1016/0043-1648\(61\)90002-3](https://doi.org/10.1016/0043-1648(61)90002-3)
 7. Tressia, G., Penagos, J.J., Sinatora, A.: Effect of abrasive particle size on slurry abrasion resistance of austenitic and martensitic steels. *Wear* (2017). <https://doi.org/10.1016/j.wear.2017.01.073>
 8. Andrade, M., Martinho, R.P., Silva, F., Alexandre, R., Baptista, A.: Influence of the abrasive particles size in the micro-abrasion wear tests of TiAlSiN thin coatings. *Wear* (2009). <https://doi.org/10.1016/j.wear.2008.12.114>
 9. Dwyer-Joyce, R.S., Sayles, R.S., Ioannides, E.: An investigation into the mechanisms of closed three-body abrasive wear. *Wear* (1994). [https://doi.org/10.1016/0043-1648\(94\)90176-7](https://doi.org/10.1016/0043-1648(94)90176-7)
 10. Ren, X., Peng, Z., Hu, Y., Rong, H., Wang, C., Fu, Z., Qi, L., Miao, H.: Three-body abrasion behavior of ultrafine WC–Co hardmetal RX8UF with carborundum, corundum and silica sands in water-based slurries. *Tribol. Int.* (2014). <https://doi.org/10.1016/j.triboint.2014.07.008>
 11. Petrica, M., Katsich, C., Badisch, E., Kremsner, F.: Study of abrasive wear phenomena in dry and slurry 3-body conditions. *Tribol. Int.* (2013). <https://doi.org/10.1016/j.triboint.2013.03.028>
 12. Yu, R., Chen, Y., Liu, S., Huang, Z., Yang, W., Wei, W.: Abrasive wear behavior of Nb-containing hypoeutectic Fe–Cr–C hardfacing alloy under the dry-sand/rubber-wheel system. *Mater. Res. Exp.* (2019). <https://doi.org/10.1088/2053-1591/aaedf1>
 13. Salinas Ruiz, V.R., Kuwahara, T., Galipaud, J., Masenelli-Varlot, K., Hassine, M.B., Héau, C., Stoll, M., Mayrhofer, L., Moras, G., Martin, J.M., Moseler, M., de Barros Bouchet, M.-I.: Interplay of mechanics and chemistry governs wear of diamond-like carbon coatings interacting with ZDDP-additivated lubricants. *Nat. Commun.* (2021). <https://doi.org/10.1038/s41467-021-24766-6>
 14. Bhardwaj, V., Zhou, Q., Zhang, F., Han, W., Du, Y., Hua, K., Wang, H.: Effect of Al addition on the microstructure, mechanical and wear properties of TiZrNbHf refractory high entropy alloys. *Tribol. Int.* (2021). <https://doi.org/10.1016/j.triboint.2021.107031>
 15. Buling, A., Zerrer, J.: Lifting lightweight metals to a new level—tribological improvement by hybrid surface solutions on aluminium and magnesium. *Lubricants* (2020). <https://doi.org/10.3390/lubricants8060065>
 16. Salguero, J., Vazquez-Martinez, J.M., Del Sol, I., Batista, M.: Application of pin-on-disc techniques for the study of tribological interferences in the dry machining of A92024–T3 (Al–Cu) alloys. *Materials* (Basel, Switzerland) (2018). <https://doi.org/10.3390/ma11071236>
 17. Ma, G., Wang, L., Gao, H., Zhang, J., Reddyhoff, T.: The friction coefficient evolution of a TiN coated contact during sliding wear. *Appl. Surf. Sci.* (2015). <https://doi.org/10.1016/j.apsusc.2015.03.156>
 18. Azad, K., Rasul, M.G., Khan, M., Sharma, S.C.: Ecofuel and its compatibility with different automotive metals to assess diesel engine durability. In: *Advances in Eco-Fuels for a Sustainable Environment*, pp. 337–351. Elsevier (2019). <https://doi.org/10.1016/B978-0-08-102728-8.00012-7>
 19. Li, Y., Schreiber, P., Schneider, J., Greiner, C.: Tribological mechanisms of slurry abrasive wear. *Friction* (2022). <https://doi.org/10.1007/s40544-022-0654-1>
 20. Deshpande, P., Pandiyan, V., Meylan, B., Wasmer, K.: Acoustic emission and machine learning based classification of wear generated using a pin-on-disc tribometer equipped with a digital holographic microscope. *Wear* (2021). <https://doi.org/10.1016/j.wear.2021.203622>
 21. Mindivan, H., Tekmen, C., Dikici, B., Tsunekawa, Y., Gavali, M.: Wear behavior of plasma sprayed composite coatings with in situ formed Al₂O₃. *Mater. Des.* (2009). <https://doi.org/10.1016/j.matdes.2009.05.018>
 22. Richardson, R.: The wear of metals by relatively soft abrasives. *Wear* (1968). [https://doi.org/10.1016/0043-1648\(68\)90175-0](https://doi.org/10.1016/0043-1648(68)90175-0)
 23. Williams, J.A., Hyncica, A.M.: Mechanisms of abrasive wear in lubricated contacts. *Wear* (1992). [https://doi.org/10.1016/0043-1648\(92\)90204-L](https://doi.org/10.1016/0043-1648(92)90204-L)
 24. zum Gahr, K.-H.: *Microstructure and wear of materials*. Tribology Series, vol. 10. Elsevier, Amsterdam, New York (1987)
 25. Ren, Y., Jia, Q., Du, Y., Zhou, Q., Greiner, C., Hua, K., Wang, H., Wang, J.: A wear-resistant metastable CoCrNiCu high-entropy alloy with modulated surface and subsurface structures. *Friction* (2022). <https://doi.org/10.1007/s40544-022-0606-9>
 26. Raja, J., Muralikrishnan, B., Fu, S.: Recent advances in separation of roughness, waviness and form. *Precis. Eng.* (2002). [https://doi.org/10.1016/S0141-6359\(02\)00103-4](https://doi.org/10.1016/S0141-6359(02)00103-4)
 27. Al-Samarai, R.A., Haftirman, K.R.A., Al-Douri, Y.: The influence of roughness on the wear and friction coefficient under dry and lubricated sliding. *Int. J. Sci. Eng. Res.* **3**, 1–6 (2012)
 28. Kubiak, K.J., Liskiewicz, T.W., Mathia, T.G.: Surface morphology in engineering applications: Influence of roughness on sliding and wear in dry fretting. *Tribol. Int.* (2011). <https://doi.org/10.1016/j.triboint.2011.04.020>
 29. Shi, R., Wang, B., Yan, Z., Wang, Z., Dong, L.: Effect of surface topography parameters on friction and wear of random rough surface. *Materials* (Basel, Switzerland) (2019). <https://doi.org/10.3390/ma12172762>
 30. Liang, G., Schmauder, S., Lyu, M., Schneider, Y., Zhang, C., Han, Y.: An investigation of the influence of initial roughness on the friction and wear behavior of ground surfaces. *Materials* (Basel, Switzerland) (2018). <https://doi.org/10.3390/ma11020237>
 31. Chang, W.-R., Grönqvist, R., Hirvonen, M., Matz, S.: The effect of surface waviness on friction between neolite and quarry tiles. *Ergonomics* (2004). <https://doi.org/10.1080/00140130410001670390>
 32. Archard, J.F.: Contact and rubbing of flat surfaces. *J. Appl. Phys.* (1953). <https://doi.org/10.1063/1.1721448>
 33. Prost, J., Boidi, G., Lebersorger, T., Varga, M., Vorlaufer, G.: Comprehensive review of tribometer dynamics-cycle-based data analysis and visualization. *Friction* (2022). <https://doi.org/10.1007/s40544-021-0534-0>
 34. Hsiao, E., Kim, S.H.: Analyzing periodic signals in rotating pin-on-disc tribotest measurements using discrete Fourier transform algorithm. *Tribol. Lett.* (2009). <https://doi.org/10.1007/s11249-009-9462-2>
 35. Godfrey, D.: Friction oscillations with a pin-on-disc tribometer. *Tribol. Int.* (1995). [https://doi.org/10.1016/0301-679X\(95\)92701-6](https://doi.org/10.1016/0301-679X(95)92701-6)
 36. Dai, L., Sorkin, V., Zhang, Y.W.: Probing the surface profile and friction behavior of heterogeneous polymers: a molecular dynamics study. *Modelling Simul. Mater. Sci. Eng.* (2017). <https://doi.org/10.1088/1361-651X/aa5bdf>
 37. Stachowiak, G.W., Batchelor, A.W. *Engineering tribology*. Butterworth-Heinemann (2013)
 38. Röttger, M.C., Sanner, A., Thimons, L.A., Junge, T., Gujrati, A., Monti, J.M., Nöhring, W.G., Jacobs, T.D.B., Pastewka, L.: Contact.engineering—Create, analyze and publish digital surface twins from topography measurements across many scale. *Surf. Topogr.* (2022). <https://doi.org/10.1088/2051-672X/ac860a>